Published in final edited form as:
Bioconjug Chem. 2009 October 21; 20(10): 1869–1878. doi:10.1021/bc900065r.

PEPTIDE TARGETING OF PLATINUM ANTI-CANCER DRUGS

Margaret W. Ndinguri[†], **Rajasree Solipuram**[‡], **Robert P. Gambrell**[§], **Sita Aggarwal**[*,‡], **William Hansel**[‡], and **Robert P. Hammer**[*,†,‖]

[†] Department of Chemistry, Louisiana State University, Baton Rouge, LA 70803

[‡] William Hansel Cancer Prevention Laboratory, Pennington Biomedical Research Center, Baton Rouge, LA 70808

[§] Department of Oceanography and Coastal Sciences, Louisiana State University, Baton Rouge, LA 70803

[‖] New England Peptide, Gardner, MA 01440

Abstract

Besides various side effects caused by platinum anticancer drugs, they are not efficiently absorbed by the tumor cells. Two Pt-peptide conjugates; cyclic mPeg-CNGRC-Pt (**7**) and cyclic mPeg-CNGRC-Pten (**8**) bearing the Asn-Gly-Arg (NGR) targeting sequence, a malonoyl linker and low molecular weight miniPEG groups have been synthesized. The platinum ligand was attached to the peptide via the carboxylic end of the malonate group at the end of the peptide. The pegylated peptide is non toxic and highly soluble in water. Platinum conjugates synthesized using the pegylated peptides are also water soluble with reduced or eliminated peptide immunogenicity. The choice of carboplatin as our untargeted platinum complex was due to the fact that malonate linker chelates platinum in a manner similar to carboplatin. Cell toxicity assay and competition assay on the PC-3 cells (CD13 positive receptors) revealed selective delivery and destruction of PC-3 cells using targeted Pt-peptide conjugates **7** and **8** significantly more than untargeted carboplatin. Platinum uptake on PC-3 cells was 12-fold more for conjugate **7** and 3-fold more for conjugate **8** compared to the untargeted carboplatin indicating selectively activation of the CD13 receptors and delivery of the conjugates to CD13 positive cells. Further analysis on effects of conjugates **7** and **8** on PC-3 cells using caspase-3/7, fluorescence microscopy and DNA fragmentation confirmed that the cells were dying by apoptosis.

Introduction

Platinum compounds are widely used in cancer chemotherapy (1,2). Cisplatin is an FDA-approved drug that is widely used for treatment of many types of cancers including lung, ovarian, as well as head and neck cancer (3,4). Carboplatin, an analogue of cisplatin, is being used more often because it has decreased non-specific toxicity and is active against cisplatin-resistant tumors (2,5-7). Both carboplatin and cisplatin have been shown to form similar adducts with DNA by the formation of covalent bonds with the N7 of purine bases. This results in interference with normal transcription and DNA replication mechanisms leading to eventual cell death. While these drugs are effective, they have very serious side effects that include nephrotoxicity, myelotoxicity, neurotoxicity, vomiting and nausea (8).

[*] Authors to whom all the correspondence, proof, and request for reprints should be addressed. robert.hammer@newenglandpeptide.com Sita.Aggarwal@pbrc.edu .

Supporting information available Supplemental information on ^{1}H NMR, crystal structure, HPLC analysis spectra and fluorescence microscopy images. This information is available free of charge via the internet at http://pubs.acs.org.

Certain cancers can also develop resistance to drugs like cisplatin via efflux pumps as reported by Katano *et al*. (9,10).

One method to make toxic drugs more effective is by incorporation of a cell-specific targeting group. A number of peptide sequences are capable of mediating the delivery of therapeutic or imaging drugs (11,12). Using phage display libraries, several peptide sequences that have the ability to target tumors have been discovered (13,14). The Asn-Gly-Arg (NGR) motif was identified as a peptide that uniquely homed specifically to solid tumors in murine breast carcinoma models and that bound strictly to the endothelium of angiogenic blood vessels (15). Besides the NGR motif, other peptide sequences like Arg-Gly-Asp (RGD) and luteinizing hormone releasing hormone (LHRH) have been used to target specific receptors found mainly in certain tumor cells (16-20). The NGR motif may be superior to the RGD-related motif for targeting, due to the many types of cells that express the $\alpha v\beta_3$ and $\alpha v\beta_5$ integrins that bind RGD-type sequence, which may lead to nonspecific targeting and toxicity (14). Recently, doxorubicin (DOX) and 5-fluoro-2′-deoxyuridine (5-FdUrd) conjugates have successfully been targeted using NGR motif (21,22). Specifically, DOX-peptide conjugate treated animals had increased life expectancies relative to animals treated with DOX alone (23) and a 5-FdUrd-NGR conjugate produced selective accumulation of 5-FdUrd in tumor cells having CD 13 receptors (24). Haubner *et al*. revealed that radiolabeled RGD peptide was found to concentrate rapidly in the liver, which can lead to liver toxicity in drugs that are based on RGD targeting, hence limiting the usefulness of these drugs(14).

New blood vessels are required for tumor growth (15,25). Thus, around solid-tumors angiogenesis is stimulated and endothelial cells proliferate to form new blood sources to support the growing tumor. Modulating the growth of blood vessels is one of the effective ways to control the growth and spread of tumors. Therefore, the search for targets that can regulate angiogenesis is important. Aminopeptidase N (APN), also referred to as CD13, is a cell-surface antigen that binds specifically to NGR peptides (26,27). CD13/APN is expressed selectively on the endothelial cells of angiogenic tissues and the vasculature of various carcinomas including kidney, colon, pancreas, prostate and lung (28-31). It is not expressed in normal vasculature, which explains the tumor-specific destination of the NGR peptide (3,32).

By conjugating the water-soluble cyclic peptide CNGRC to the conventional drugs cisplatin and dichloro(ethylenediamine)platinum(II) ($PtenCl_2$), we hypothesized that we could increase specificity for CD13-expressing cancerous tissues, and reduced toxicity to normal tissues. In this work, we describe the preparation of several malonoyl CNGRC peptides and their platinum conjugates and evaluate their specific targeting on tumor cells with CD13 receptors.

EXPERIMENTAL SECTION

All starting reagents listed below were obtained from commercial sources and used without further purification: Di-tert-butyl malonate, dry solvents, $AgNO_3$, 3-bromopropylphthalimide, dichloro(ethylenediamine)platinum(II), cis-diammineplatinum(II) dichloride and glutaric anhydride were obtained from Aldrich (Milwaukee WI); Fmoc-11-amino-3,6,9-trioxaundecanoic acid (miniPEG, $mPEG_3$) was obtained from Peptides International (Louisville, KY), and all amino acids were from Novabiochem (Gibbstown, NJ).

NMR Spectroscopy

^{1}H NMR spectra were recorded on either 300 or 400 MHz spectrometers. Peak positions are referenced to TMS. All NMR data were processed with *XWINNMR* and *Mestre-C* software.

HPLC

HPLC was performed using a Water 600E multisolvent delivery system with a model 486 tunable detector controlled by Empower software and Water Deltaprep system, with detection at 220 nm. Different columns were used for analysis and purification of the peptides. Analytical and semi-preparative chromatography was performed on a Delta-Pak C_4 (5 μm; 100 Å) reverse phase column (8 × 100 mm) at 1 mL/min (Column 1). Preparative HPLC was performed on Waters Delta-Pak C_4 (15 μm; 100 Å) reverse phase column (25 × 100 mm) at 15 mL/min (Column 2). Linear gradients of 0.1% TFA in H_2O (Eluent A) and 0.1% TFA in MeCN (Eluent B) in all HPLC were used.

Mass Spectrometry

Compounds were analyzed using ESI on an Agilent Technologies instrument processed with Analyst QS1.1 (Applied Biosystems) or Mass Hunter (Agilent).

Inductive Coupled Plasma-Optical Emission Spectroscopy

Platinum uptake was analyzed using a Varian, Vista MPX CCD simultaneous spectrometer. PlasmaCal Pt (1000 μg/ml) from SCP Science was used for calibration by diluting it to standard solutions of known concentration.

Synthesis

Peptide Synthesis

All peptides were synthesized using standard Fmoc solid phase chemistry. Fmoc-PAL-PEG-PS (Peptide Amide Linker resin: 0.2 mmol, 0.24 mmol/g loading) was placed in a normal resin column and washed with DMF in continuous flow mode using a Pioneer Peptide Synthesizer. The side chain-protected amino acid derivatives used in the sequence were Fmoc-Cys(Acm)-OH, Fmoc-Arg(Pbf)-OH, Fmoc-Gly-OH, Fmoc-Asn(Trt)-OH and Fmoc-Cys(Acm)-OH. Fmoc-mini-peg-3™ and the derivatized malonate linker di-tert-butyl 2-(3-glutaricaminopropyl)malonate were also used, depending on the peptide sequence. All couplings utilized four equivalents each of amino acids, malonate and PyAOP (33) dissolved in 0.5 M DIEA in DMF (final concentration being 0.25 M) for 1 hour at room temperature; minimal preactivation time was used in the coupling. DMF was used for washing between coupling and deprotection cycles. The Fmoc group was removed using 20% piperidine in DMF for 5 min. Final washing was with DMF and dichloromethane.

Synthesis of CNGRC-Mal (1)

In an attempt to synthesize CNGRC-Mal, we synthesized cyclic CNGRC using the method described by Anizon *et al*. using NovaSyn TGT alcohol resin (0.20 mmol, 0.20 mmol/g loading) (23). Conjugation of CNGRC with di-tert-butyl 2-(3-aminopropyl)malonate was unsuccessful (Scheme 1).

Synthesis of Mal-Glut-CNGRC (2)

Using standard Fmoc chemistry, we synthesized Mal-Glut-CNGRC using the procedure described in the peptide synthesis section, using PAL-PEG-PS resin without the Fmoc-mini-peg-3™ solubilizing group. Coupling the peptide with di-tert-butyl 2-(3-glutaricaminopropyl)malonate gave crude Mal-Glut-CNGRC peptide, which was purified by reverse phase HPLC on column 1 using a linear gradient from 5% to 70% B eluent in 60

min, t_R 11 min. The adduct gave the expected $(M+H)^+$ Peak at 807.2893, calculated for $C_{29}H_{48}N_{11}O_{12}S_2$ 807.2925 (see supporting information). Using the procedure described for the preparation of cyclic mPeg-CNGRC-Pt, the peptide was reacted with cis-$[Pt(NH_3)_2(H_2O)_2]^{2+}(NO_3)_2$ to give an insoluble yellow solid (Scheme 2) which was not suitable for further characterization.

Synthesis of Di-tert-butyl 2-(3-Phthalimidopropyl)malonate (3)

Di-tert-butyl 2-(3-phthalimidopropyl)malonate was synthesized by a known method (Scheme 3) with slight modifications (34). NaH (0.38 g, 16 mmol) was suspended in dry THF (100 mL), and dry di-tert-butyl malonate (4.4 mL, 20 mmol) was added to the reaction mixture (with stirring) until gas evolution ceased. A solution of 3-bromopropylphthalimide (2.68 g, 10 mmol) was added drop-wise to the reaction mixture, followed by stirring overnight. The THF was removed by evaporation, and the product was re-dissolved in CH_2Cl_2 and washed with 5% aqueous acetic acid. The organic fractions were combined, dried over $MgSO_4$ and concentrated. The final product was isolated using silica column chromatography (95% Hexane, 5% ethyl acetate). Di-tert-butyl 2-(3-phthalimidopropyl)malonate was crystallized using a mixture of CH_2Cl_2 and hexane to give colorless plates (see supporting information). The yield was 80% (3.22 g). Spectroscopic data obtained for this compound were in agreement with literature values (34).

Synthesis of Di-tert-butyl 2-(3-aminopropyl)malonate (4)

Compound **4** was prepared by known method as described by Aronov *et al*. (34). Di-tert-butyl 2-(3-phthalimidopropyl)malonate was deprotected using absolute hydrazine to give di-tert-butyl 2-(3-aminopropyl)malonate. The ^1H NMR spectrum of compound **4** (Scheme 3) in $CDCl_3$ matched the reported values.

Synthesis of Di-tert-butyl 2-(3-(4-carboxybutanamido)propyl)malonate (5)

Compound **5** was synthesized as previously described in the literature (34). Glutaric anhydride was used for acylation in this reaction yielding the glutaroyl(aminopropyl)malonic ester **5** (Scheme 3). The yield was 92%.^1H NMR ($CDCl_3$) (ppm): 3.27 (q, 2H), 3.14 (t, 1H), 2.41 (t, 2H), 2.28 (t, 2H), 1.98 (m, 2H), 1.81(m, 2H), 1.56 (m, 2H), 1.45(s, 18H).

Synthesis of cyclic mPeg-CNGRC-mal (6)

After synthesizing the linear mPeg-CNGRC-mal peptide, and confirming its purity, the resin was suspended in DMF (60 mL) and the reaction mixture cooled to 0 °C in an ice bath before the addition of I_2 (10 equiv). The mixture was stirred at 0 °C for 2 h, filtered and washed with DMF (10 × 10 mL) and CH_2Cl_2 (10 × 10 mL). Using a cocktail of TFA:phenol:water:TIPS (88:5:5:2) (15 mL), the peptide was cleaved from the resin, precipitated with ether and dried under vacuum to give crude peptide **6**. The crude peptide was purified using reverse phase HPLC on column 1 with a linear gradient from 5% to 70% B eluent in 60 min, t_R 28 min. This yielded cyclic mPeg-CNGRC-mal (**6**) in 35% yield. ESI-MS (TOF) gave a signal at 1184.4764 $(M + H)^+$, calculated for $C_{45}H_{77}N_{13}O_{20}S_2$ 1184.4849 (see supporting information).

Synthesis of cyclic mPeg-CNGRC-Pt (7)

Cyclic mPeg-CNGRC-mal was dissolved in water and the pH of the solution was adjusted to 7, by titration with 1M NaOH (See supporting information). A solution of cis-$[Pt(NH_3)_2(H_2O)_2]^{2+}(NO_3)_2$ was made by stirring cis-$PtCl_2(NH_3)_2$ and $AgNO_3$ vigorously overnight in water in the dark. A precipitate was formed (AgCl) and then filtered to give cis-$[Pt(NH_3)_2(H_2O)_2]^{2+}(NO_3)_2$ (35, 36). A 2-fold excess of cis-$[Pt(NH_3)_2(H_2O)_2]^{2+}(NO_3)_2$ (10

mmol) was reacted with compound **6** (30 mg, 5 mmol) to form the crude cyclic mPeg-CNGRC-Pt conjugate (**7**), which was then purified by gel filtration on Sephadex-G10 column to give the final product in 15% yield. ESI-MS (TOF) gave a signal at 1412.4913 $(M + H)^+$, calculated for $C_{45}H_{81}N_{15}O_{20}PtS_2$ 1412.4955 (see supporting information).

Synthesis of cyclic mPeg-CNGRC-Pten (8)

Cyclic mPeg-CNGRC-mal was dissolved in water and the pH of the solution was adjusted to 7, by titration with 1M NaOH. Cis-$[Pten(H_2O)_2]^{2+}(NO_3)_2$ was synthesized by stirring $PtenCl_2$ and $AgNO_3$ vigorously overnight, in water in the dark. A precipitate was formed (AgCl) and then filtered to yield cis-$[Pten(H_2O)_2]^{2+}(NO_3)_2$ (37-39). A 2-fold excess of cis-$[Pten(H_2O)_2]^{2+}(NO_3)_2$ (10 mmol) was reacted with compound **6** (30 mg, 5 mmol) to give crude cyclic mPeg-CNGRC-Pten conjugate, which was then purified by gel filtration on Sephadex-G10 column to give cyclic mPeg-CNGRC-Pten **(8)** in 10-12% yield. ESI-MS (TOF) gave a signal at 719.7571 $(M + H)^{2+}$, calculated for $C_{47}H_{83}N_{15}O_{20}PtS_2$ 719.7593 (see supporting information).

Synthesis of cyclic mPeg-CNGRC (9)

Free peptide (**9**) was assembled as described in the peptide synthesis section, without the malonate linker **5**. The crude peptide was purified by reverse phase HPLC on column 1 with a linear gradient from 5% to 70% B eluent in 60 min, t_R 10 min to give cyclic mPeg-CNGRC (**9**) in 38% yield. ESI-MS (TOF) gave a signal at 927.4032 $(M + H)^+$, calculated for $C_{34}H_{62}N_{12}O_{14}S_2$ 927.4023 (see supporting information).

Cell culture

The prostate cancer cell line PC-3 (CRL-1435) was obtained from the American Type Culture Collection (Manassas, VA). Penicillin, streptomycin, RPMI 1640, and fetal bovine serum (FBS) were obtained from Invitrogen (Grand Island, NY). The cell line was cultured in RPMI 1640 supplemented with 10% FBS, 100 units/mL penicillin, and 100 μg/mL streptomycin.

Fluorescence microscopy

PC-3 cells were seeded on 6-well plates (500,000 cells/well) and incubated for 24 h in RPMI 1640 media. The cells were treated with 200 μM of carboplatin, a mixture of carboplatin and free peptide **9**, or Pt-peptide conjugates **7** or **8** for 48 h. After incubation, the cells were washed once with RPMI and stained with JC-1 dye for 30 min. The stained cells were analyzed using a Leica DM RXA fluorescent microscope with Xenon lamp illumination, using a 40 × dip objective with an N.A. of 0.80. The filter cube for the green channel had the following characteristics: a 480/40 excitation filter, a 527/30 emission filter and a 505 nm dichroic mirror. The filter cube used for the red channel had the following characteristics: a 537/45 excitation filter, an LP 590 emission filter, and a 580 nm dichroic mirror.

Cytotoxicity assay

The cytotoxicity of the free carboplatin, free peptide cyclic mPeg-CNGRC-mal (**6**), the mixture of carboplatin and mPeg-CNGRC (**9**) as well as the two platinum conjugates (cyclic mPeg-CNGRC-Pt (**7**) and cyclic mPeg-CNGRC-Pten (**8**)) was assayed using the MTT (3-(4, 5-dimethylthiazol-2-yl)-2, 5-diphenyltetrazolium bromide) assay as described (40). Briefly, 2000 cells/well were incubated in 96-well plates in triplicate, using different concentrations of platinum complexes in a cell growth medium. Three wells were used as controls, receiving an equivalent volume of RPMI medium alone. The cells were treated with different concentrations (0 μM, 50 μM, 150 μM, 200 μM and 300 μM) of carboplatin, free peptide **6**, the mixture of carboplatin and mPeg-CNGRC (**9**) and the Pt-peptide conjugates **7**

and **8** for 48 h. After 48 h, a solution of MTT (5 mg/ml in PBS) was added to each well, and the cells were incubated for 2 h at 37 °C. The cells were then lysed using a lysis buffer (20% SDS and 50% DMSO). The lysed cells were incubated for 3 h at 37 °C, before the absorbance of the cell suspension was measured at 590 nm using an MRX Revelation 96-well multiscanner (Dynex Technologies, Chantilly, VA).

Drug competition assay

Using various concentrations of mPeg-CNGRC (**9**), a cell competition assay for carboplatin and conjugates **8** was carried out using the MTT assay. 2,000 cells/well were incubated in 96-well plates one day prior to the treatment to allow the cells to adhere to the plate in triplicate. On the next day the cells were treated using various concentrations of the free peptide mPeg-CNGRC (**9**) (1 mM, 2 mM, 4 mM, 8 mM and 10 mM) followed by the addition of 200 μM of carboplatin and conjugate **8** for 48 h. The plate was analyzed as described in the cell cytotoxicity assay.

Drug uptake measurements

One million PC-3 cells were plated in a 6-well plate a day before for adherence. On the next day, the cells were treated with fresh medium containing 200 μM carboplatin, and Pt-peptide conjugates **7** and **8** for 24 h. After incubation, the cells were washed with PBS once and collected in a tube for further analysis. The collected samples were dissolved in 0.25 ml nitric acid (trace metal grade) and heated for 2 h at 60 °C for digestion. Upon cooling, approximately 5 mL of deionized water was added to dilute the samples to the minimum volume required for the ICP spectrometer.

The apo-ONE homogenous caspase-3/7 assay

The homogenous caspase-3/7 assay kit (Promega, Madison, WI), which provides a profluorescent substrate with an optimized bifunctional cell lysis/activity buffer for caspase-3/7 activity assays, was used. PC-3 cells were treated with free peptide **9**, or a mixture of free peptide **9** and carboplatin, conjugate **7** or conjugate **8** at 100 μM concentration. After 24 h of incubation, apo-ONE homogenous caspase-3/7 assay was performed according to the manufacturer's protocol. The buffer and substrate were mixed and added to the samples. Upon sequential cleavage and removal of the DEVD (Asp-Glu-Val-Asp) peptides by caspase-3/7 activity and excitation at 499 nm, the rhodamine 110 leaving group became intensely fluorescent with emission maximum at 512 nm (41). The excitation/emission was recorded on FlexStation from Molecular Devices (Sunnyvale, CA) with softMax Pro version 4.8 software. This experiment was performed in duplicate and the statistical analysis was done.

DNA fragmentation assay

The evaluation of nuclear morphological event such as internucleosomal DNA fragmentation was performed by standard agarose gel electrophoresis as described previously (42). Briefly, treated cells (one million cells) were washed in ice-cold PBS, resuspended in 0.2 ml PBS in 1.5 ml Eppendorf tubes. Next 0.2 ml of lysis buffer (20 mM Tris-HCl, pH 7.4, 1% triton x-100.10 mM EDTA, 0.1 mg/ml proteinase K) was added and the mixture was incubated at 55 °C for 2 h. Proteinase K was then heat inactivated at 70 °C for 10 min and the sample was cooled to room temperature. RNAse was added (10 μl of 20 mM Tris–HCl pH 7.4 containing 0.5 mg/ml RNase) to the sample which was further incubated for 2 h at 37 °C. Extraction of DNA was achieved with 1:1 mixture of phenol: chloroform and precipitated with two volumes of cold ethanol and one-tenth volume of sodium acetate. The sample was centrifuged and the pellet was resuspended in 50 μl of deinonized water. Samples were loaded on a 1.5% agarose gel and electrophoresed at 60 V

for 2 h in TBE. The gel was stained with EtBr and visualized by UV trans-illumination using a Bio-Rad Versa Doc Imaging system (Model 3000).

Results and discussion

In order to evaluate the optimal construct for delivering a platinum-peptide conjugate, several CNGRC-chelator constructs were evaluated. Figure 1 shows the two designs that we tested for the formation of Pt-peptide complexes, with design B being the more successful of the two. Design A was based on attaching the chelator to the C-terminus of the peptide acid as had been done for DOX-NGR conjugate. (23) Design B has the linker attached to the N-terminus, which has potential advantages for incorporation by solid-phase synthesis.

Following Design A, our initial attempt was to couple the cyclic CNGRC peptide with di-tert-butyl 2-(3-aminopropyl)malonate using solution phase chemistry by conjugating the free carboxylic end of the cysteine with the free amine end of di-tert-butyl 2-(3-aminopropyl)malonate (Scheme 1). The cyclic CNGRC peptide was prepared as described by Anizon *et al*. (23), where the trityl alcohol resin was converted to the trityl chloride derivative with acetyl chloride. This was followed by loading of the Fmoc-Cys(Acm)-OH onto resin resulting in a 0.14 mmol/g (70%) loading yield. The resin was treated with Fmoc-Arg(Pbf)-OH, Fmoc-Gly-OH, Fmoc-Asn(Trt)-OH, and Fmoc-Cys(Acm)-OH to give crude CNGRC. The HPLC chromatogram and the mass spectrum revealed the expected $(M + H)^+$ peak at 550.76, which was in agreement with the reported values. Di-tert-butyl 2-(3-aminopropyl)malonate was prepared as described in the experimental section using a slight modification of the Aronov method (34). The malonate was alkylated using a strong base to give product in 80% yield. A similar synthesis was achieved by the Aronov group using KOt-Bu as a base; however, using a stronger base (NaH) in the reaction improved the yields from 60% to 80% yield. A 2-fold excess of di-tert-butyl malonate was used to ensure monoalkylation and the ease of separation between the malonate and di-tert-butyl 2-(3-phthalimidopropyl)malonate. The excess of the di-tert-butyl malonate that was used was easily removed by column chromatography (34). Attempts to couple the cyclic peptide CNGRC and di-tert-butyl 2-(3-aminopropyl)malonate (Scheme 3) using various coupling reagents were unsuccessful (Scheme 1). We do not understand why the reaction failed as similar reactions between CNGRC and DOX with similar functional groups have been successful (23). Analysis of the crude product revealed high amounts of the starting materials, including CNGRC, di-tert-butyl 2-(3-aminopropyl)malonate, and coupling reagents.

In order to overcome the above problem we explored Design B. This enabled us to conjugate the linker on the N-terminus of peptide resin, thereby avoiding solution phase chemistry in the conjugation of the linker-chelator group to the peptide CNGRC, as shown in Scheme 2. To achieve this synthesis, malonate linker with a carboxylic acid end (**5**) was synthesized using glutaric anhydride and di-tert-butyl 2-(3-aminopropyl)malonate (**4**), as shown in Scheme 3. Starting from an amide-based resin and using Fmoc chemistry, the peptide was assembled and then conjugated to di-tert-butyl 2-(3-glutaricaminopropyl)malonate and cyclized on the solid support to yield Mal-Glut-CNGRC. After purification, HPLC and mass spectral analysis confirmed the purity and identity of the cyclic Mal-Glut-CNGRC. Platination of the purified Mal-Glut-CNGRC using cis-$[Pt(NH_3)_2(H_2O)_2]^{2+}(NO_3)_2$ gave an insoluble yellow compound in most solvents, including water, DMSO, DMF, MeOH, acetone, MeCN, CH_3Cl, and CH_2Cl_2. The compound could not be characterized by mass spectra to confirm the formation of platinum complex.

Our third and final approach was to increase the solubility of the CNGRC sequence by adding short oligomeric PEG-based residues to both the N- and C-termini of the peptide.

Additionally, the PEG linker would provide additional spacing of the Pt-ligand from the targeting peptide. Various studies have shown that pegylation does not affect targeting and may have other positive effects such as an increase in stability that reduces the chance of the drug efflux (34), and it reduces or eliminates immunogenicity (43-45). We chose the $mPEG_3$ derivative as the spacer as it is conveniently available as an Fmoc-protected amino acid derivative. The peptide was prepared as before adding on these residues at each terminus. The glutaric anhydride and linker-malonate were added at the N-terminus and the linear peptide was cyclized on solid support and cleaved to give target compound **6** (Scheme 4) which was purified by HPLC and its identity was confirmed by mass spectroscopy (see supporting information).

Peptide-Platinum complexes

Platination with a 2-fold excess of activated cis-$[Pt(NH_3)_2(H_2O)_2]^{2+}(NO_3)_2$ and cis-$[Pten(H_2O)_2]^{2+}(NO_3)_2$ using a standard procedure gave Pt-Peptide conjugates **7** and **8** as shown in Scheme 4. The platinum complexes could not be purified by HPLC using either an acidic or a neutral buffer system because the platinum complexes dissociated. The products were therefore purified by gel filtration to remove the excess platinum. Fractions containing the Pt-peptide complex in water were identified by ESI-MS and then combined and lyophilized to give pure platinum complexes for cyclic mPeg-CNGRC-Pt (**7**) and cyclic mPeg-CNGRC-Pten (**8**) in a 10-15% yield. Mass spectra revealed the expected $(M + H)^+$ peak at 1412.4913 for conjugate **7** and the $(M + 2H)^{2+}$ peak at 719.7571 for conjugate **8**. During the study, we noticed that platinum conjugate **7** was not very stable in PBS at −20 °C and formed precipitates after a day of storage. Any experiment with conjugate **7** had to use freshly dissolved conjugate. The ethylene diamine Pt conjugate **8** was stable at −20 °C, and the stock solutions could be used in later experiments. Both Pt conjugates were stable as lyophilized powders at −20 °C and fresh samples were made by reconstituting the dry samples to the desired concentration. The integrity of redissolved Pt-peptide conjugates was confirmed by ESI mass spectrometry before use.

In vitro studies on Pt-conjugates: their toxicity and uptake

It has been shown that the NGR motif binds specifically to the CD13 receptors that are expressed on some tumor cells. We examined the effect of the free peptide as a control experiment to determine the effect of the peptide. As shown in Figure 2, the free peptide (**6**) was not toxic to the PC-3 cells and caused a slight increase in the MTT assay, suggesting that the PC-3 receptors were activated by the NGR ligand. Two CNGRC platinum conjugates were prepared to test our hypothesis. As expected, the targeted Pt-peptide conjugates **7** and **8** were more toxic to the PC-3 cells at all concentrations tested compared to the untargeted carboplatin (even at concentrations as low as 50 μM). Pt-conjugate **8** shows the highest effect on the suppression of cell proliferation, followed by Pt-conjugate **7** and carboplatin. Carboplatin was the least toxic to PC-3 cells of this series of platinum compounds, indicating that the platinum complexes bearing the CNGRC sequence are more effective at suppressing tumor cell proliferation. The % growth inhibition on PC-3 cells caused by the mixture of mPeg-CNGRC (**9**); (peptide not bearing a Pt-chelating group) and carboplatin was similar to that caused by carboplatin alone, suggesting that there was no effect of the peptide on the toxicity of carboplatin. At 150 μM, less than 50% of the PC-3 cells were viable when exposed to the targeted Pt-peptide conjugates, compared to greater than 60% for the untargeted carboplatin drug. A concentration of 200 μM showed the most substantial effect on cell proliferation (Figure 2). These results suggest that higher uptake of Pt leads to greater suppression of the proliferation of PC-3 cells. Our results are in agreement with the other groups, who have shown that CNGRC motif contributes to the increased intracellular concentration of drugs that are attached to this motif, due to targeting

to CD13 positive cells. A 5-FdUrd conjugate bearing the homing peptide CNGRC was found to penetrate into the CD13 positive cells (HT-1080) but not in CD13 negative cells (MDA-MB-231). This enhanced the selective accumulation of 5-FdUrd, resulting in a more effective immunotherapy (24). IC_{50} values for conjugate **7** and conjugate **8** are 149 μM and 115 μM respectively.

Competition assay

Figure 3 demonstrates that the free peptide **9** had no cytotoxic effect on the PC-3 cells and can effectively compete off the NGR-Pt conjugate toxicity by simultaneous incubation of the free peptide **9** and conjugate **8**. A slight increase in the % viability with peptide **9** suggests the activation and nourishment of the PC-3 cells. The use of free peptide **9** instead of free peptide **6** was to ensure that carboplatin was not chelated by the free peptide **6** which has free malonate group that is capable of reacting with the hydrolyzed carboplatin to give ambiguous results. Carboplatin and conjugate **8** were incubated with various concentration of free peptide **9**. Incubation of carboplatin with various concentration of free peptide **9** had the same effect on the % viability irrespective of the amount of free peptide **9** used. Incubation of conjugate **8** with various concentrations of free peptide **9** showed that the free peptide was competing with conjugate **8** in targeting the CD13 receptors. With an initial 5-fold excess of free peptide **9**, conjugate **8** was more cytotoxic than free carboplatin, but with a 10-fold excess, the free peptide **9** was able to compete away the effect of conjugate **8** in comparison to carboplatin. A further 50-fold increase in the free peptide concentration resulted in the elimination of the cytotoxic effect from conjugate **8**. The results also demonstrate that the CNGRC motif contributes to the accumulation of platinum in the tumor cells, causing a significant difference in the suppression of the proliferation of PC-3 tumor cells.

High uptake seems related to the toxicity of Pt-peptide conjugates **7** and **8**, supporting the hypothesis that high uptake of platinum drugs results in high cytotoxicity. When other targeting ligands have been used, platinum uptake in some cell lines show comparable values and trends closely related to our results, where targeted drugs had a higher uptake than untargeted platinum drugs (46-49). To our surprise, even though the uptake of Pt-peptide conjugate **8** was lower than that of Pt-peptide conjugate **7**, conjugate **8** was more toxic than conjugate **7**. This suggests that either the activation mechanism or the delivery pathway of conjugates **7** and **8** might be different. Clinical trials of ethylenediamine platinum complexes were suspended, as previous animal studies have shown high nephrotoxicity relative to cisplatin (50,51). Our findings suggest that targeting of the Pten conjugate **8** may be a mechanism to reduce the non-specific toxicity of this extremely potent compound. This shows that care should be taken when interpreting whether high platinum uptake has a direct relationship with cell death, and that more studies need to be done on this area. Our major concern during this experiment was to ensure that the cisplatin/carboplatin moiety detaches from the carrier at the right place at the right time. With this in mind, we chose carboplatin as our control drug in the experiment because we expected that our targeted compound would release the drug in a manner similar to carboplatin

To confirm the cell toxicity results obtained above, the uptake of platinum by PC-3 cells was determined by exposing the cells to 200 μM carboplatin, Pt-peptide conjugate **7** and Pt-peptide conjugate **8** for 24 h. The greatest Pt uptake occurred with Pt-peptide conjugate **7** followed by conjugate **8**, and the lowest uptake occurred with carboplatin, in PC-3 cells. The uptake of untargeted carboplatin was determined to evaluate the difference with the targeted complexes. From the data in Figure 4, platinum uptake by the PC-3 cells was 12-fold greater when using conjugate **7** and 3-fold greater when using conjugate **8** compared to untargeted carboplatin. These results clearly suggest that the PC-3 cells more readily take up Pt when it

is conjugated with the CNGRC-containing ligands, most likely mediated by the CD13 receptors. However, there is not a direct correlation between the amount of Pt that is taken in and how toxic the compounds are. For example, Pten complex **8** has a lower IC_{50}, but shows less uptake of platinum. Thus, the form of the Pt-complex may make a difference in the ultimate effectiveness of the drug. This may explain why the Pten complex **8** still is more toxic to the PC-3 cells than the more readily taken up Pt-amine complex **7**.

Mechanism of Action of Pt-complex toxicity

The putative mechanism of action of Pt drugs is crosslinking of nuclear DNA through reaction with the N7 of purines, there are several competing hypotheses that suggest that Pt compounds may react with effector molecules in the mitochondria that lead to apoptosis (52). We have investigated the mechanism of action of the Pt-peptide conjugates relative to carboplatin. Since it was established that both the diamino-Pt conjugate **7** and the ethylenediamino-Pt complex **8** have cellular toxicity mediated by binding to the CD13 receptor and that Pt was getting into the cells, we wanted to further establish the mechanism of action of these complexes. It is known that Pt drugs act by a variety mechanisms on cells including interaction with the mitochondria resulting in apoptosis (52,53). To determine whether Pt-peptide conjugates **7** and **8** can induce apoptosis, we used a series of experiments to further elucidate their mechanism of toxicity relative to carboplatin. We investigated various steps of the apoptotic pathway that are in response to Pt-compounds. Decrease in mitochondrial membrane potential during apoptosis, leads to the loss of outer mitochondrial membrane integrity and release of cytochrome *c* from the mitochondria. The released cytochrome *c* binds APAF1, forming an “apoptosome” that activates the apoptotic protease caspase 9, which, in turn activates downstream caspases, such as caspase 3, 6, and 7 (54), leading to the final stages of apoptosis, which is typified by DNA fragmentation.

Using the JC-1 dye that is sensitive to mitochondrial membrane potential, we qualitatively examined the action of Pt-peptide conjugates on PC-3 cells (Figure 5) by fluorescence microscopy. Image **A** shows untreated, healthy cells grown in media which have aggregated JC-1 dye concentrated in their mitochondrial membranes that give a predominantly red fluorescence. Apoptotic cells have a low membrane potential resulting in a green fluorescence which is evident in image **B.** 50% DMSO was used to induce 100% cell cytotoxicity. The results shown in Figure **C** confirmed that targeted Pt-peptides conjugate **8** (see supporting information for data on compound **7**) cause a decrease in the membrane potential, suggesting death by apoptosis in the PC-3 cell line. Images **D** and **E** show PC-3 cells treated with mixture of carboplatin/free peptide **9** (1:50) and carboplatin alone, respectively. The images show more cells with normal membrane potentials when compared to PC-3 cells treated with targeted conjugate **7** (55).

DNA fragmentation assay

The microscopy results suggest that the Pt-peptide conjugates may be acting by an apoptotic mechanism. To confirm that conjugates **7** and **8** induce internucleosomal DNA fragmentation, we incubated PC-3 cells with 100 μM each of conjugate **7** and conjugate **8** for 48 h along with appropriate controls. Result from Figure 6 clearly indicates that conjugate **7** and conjugate **8** displayed increased DNA fragmentation relative to carboplatin alone.

An intermediate step in apoptosis is the activation of caspase 9 and eventually activation of caspase 3. Figure 7 shows the results of the apo-ONE caspase assay of cells treated with Pt-peptide conjugates and carboplatin relative to controls. Treatment of the cells with carboplatin alone induces the caspase-3/7 activity significantly relative to treatment with medium alone or a non-Pt-containing peptide **9**. This result is consistent with literature

reports that anticancer Pt drugs act at least in part through an apoptotic pathway (56). Incubation of PC-3 cells with 100 μM of conjugate **7** and conjugate **8** results in significantly higher activation of caspase-3/7 relative to carboplatin treatment, which suggests stronger induction of apoptosis in PC-3 cells with the Pt-peptide conjugates. This is consistent with the DNA fragmentation assay as well as the microscopy results with JC-1 that supports targeted conjugates being much more efficient at entering and activating apoptosis than the non targeted carboplatin alone.

Beside interaction of Pt(II) compound with DNA, other effectors in the cell including mitochondrial RNA, sulfur-containing enzymes such as metallothionein and glutathione also bind to platinum (1,2). Although, much attention has been focused on the various Pt-DNA adducts formation, (57-59) their role in cytotoxicity and anti-tumor activity is still unclear (60-62). There are many studies that have described the depolarization of the mitochondrial membrane as an important characteristic of the mitochondrial or intrinsic pathway leading to apoptosis (63,64). However, data with drop in mitochondrial membrane potential is argued for and against apoptosis and therefore remains controversial (65). From the fluorescence microscopy, caspase-3/7 and DNA fragmentation data, it is clear that the intrinsic pathway is engaged through mitochondria leading to cell death but we cannot exclude extrinsic pathway. However, more studies need to be done to delineate, the exact pathway leading to apoptosis. Below is the suggested pathway that is leading to the apoptotic death of the PC-3 cells incubated with conjugate **7** and conjugate **8.**

Conclusion

Our work focused on synthesizing novel targeted Pt-peptide conjugates using the NGR motif and a malonoyl linker. The advantage of the targeted platinum analogues that we synthesized and studied in this work is that they increase the selectivity and specificity for the cancer cells and are less toxic to normal tissues. This study reveals two new low molecular weight Pt-peptide conjugates that effectively deliver the cisplatin and $PtenCl_2$ to the tumor cells, thereby increasing the toxicity towards PC-3 tumor cells. Pegylation of the peptide CNGRC allowed us to study the carrier at physiological conditions; however, the solubility problem did not allow us to compare the difference in cytotoxicity of the non pegylated. The presence of the bidentate dicarboxylate ligand in carboplatin has been shown to slow the degradation of carboplatin into potentially damaging derivatives, thereby reducing nonspecific toxicity and increasing the potency relative to cisplatin (66,67). With the aid of the miniPEG and the bidentate ligand, we show that Pt-peptide conjugates **7** and **8** which are analogues of carboplatin were able to target tumor cells that had CD13 receptors.

Supplementary Material

Refer to Web version on PubMed Central for supplementary material.

Acknowledgments

The authors would like to thank Dr. Azeem Hasan for mass spectra analysis, Martha Juban for expert technical support with peptide synthesis and purification and Dr. Matthew Brown for assistance with fluorescence microscopy. Cell Biology and Bio-imaging core at Pennington Biomedical Research Center that are supported in part by COBRE (NIH P20-RR021945) and CNRU (NIH 1P30-DK072476).

Abbreviations

PyAOP	(7-Azabenzotriazol-1-yloxy)tripyrrolidinophosphonium hexafluorophosphate
DMF	N,N-dimethylformamide

TFA	trifluoroacetic acid
DIEA	N,N-diisopropylethylamine
TIPS	triisopropylsilane
DMSO	dimethyl sulfoxide
Fmoc	fluorenylmethoxy carbonyl
PBS	phosphate-buffered saline
FBS	fetal bovine serum
ESI-MS	electrospray ionization mass spectrometry
TOF	time of flight
KOt-Bu	potassium *tert*-butoxide
PAL	5-(4-aminomethyl-3,5-dimethoxyphenoxy)valeric acid (Peptide Amide Linker)
PEG-PS	poly(ethylene glycol)-polystyrene
Pten	ethylenediamine platinum(II)

References

(1). Wang D, Lippard SJ. Cellular processing of platinum anticancer drugs. Nat. Rev. Drug Discovery 2005;4:307–320.

(2). Reedijk J. Improved understanding in platinum antitumor chemistry. Chem. Commun. (Cambridge) 1996:801–6.

(3). Shipp M, Look T. Hematopoietic Differentiation Antigens That Are Membrane-Associated Enzymes: Cutting Is the Key! Blood 1993;82:1052–1070. [PubMed: 8102558]

(4). Jamieson E, Lippard S. Structure, Recognition, and Processing of Cisplatin-DNA Adducts. Chem. Rev. (Washington, DC, U. S.) 1999;99:2467–2498.

(5). Hamelers IHL, Van Loenen E, Staffhorst RWHM, De Kruijff B, De Kroon AIPM. Carboplatin nanocapsules: a highly cytotoxic, phospholipid-based formulation of carboplatin. Mol. Cancer Ther 2006;5:2007–2012. [PubMed: 16928821]

(6). Sood P, Thurmond KB II, Jacob JE, Waller LK, Silva GO, Stewart DR, Nowotnik DP. Synthesis and Characterization of AP5346, a Novel Polymer-Linked Diaminocyclohexyl Platinum Chemotherapeutic Agent. Bioconjugate Chem 2006;17:1270–1279.

(7). Kelland LR, Murrer BA, Abel G, Giandomenico CM, Mistry P, Harrap KR. Ammine/amine platinum(IV) dicarboxylates: a novel class of platinum complex exhibiting selective cytotoxicity to intrinsically cisplatin-resistant human ovarian carcinoma cell lines. Cancer Res 1992;52:822–8. [PubMed: 1737343]

(8). Cubeddu LX, Hoffmann IS, Fuenmayor NT, Finn AL. Efficacy of ondansetron (GR 38032F) and the role of serotonin in cisplatin-induced nausea and vomiting. N. Engl. J.Med 1990;322:810–6. [PubMed: 1689807]

(9). Ghezzi A, Aceto M, Cassino C, Gabano E, Osella D. Uptake of antitumor platinum(II) complexes by cancer cells, assayed by inductively coupled plasma mass spectrometry (ICP-MS). J. Inorg. Biochem 2004;98:73–78. [PubMed: 14659635]

(10). Katano K, Kondo A, Safaei R, Holzer A, Samimi G, Mishima M, Kuo Y-M, Rochdi M, Howell SB. Acquisition of resistance to cisplatin is accompanied by changes in the cellular pharmacology of copper. Cancer Res 2002;62:6559–6565. [PubMed: 12438251]

(11). van Zutphen S, Reedijk J. Targeting platinum anti-tumour drugs: Overview of strategies employed to reduce systemic toxicity. Coord. Chem. Rev 2005;249:2845–2853.

(12). Galanski M, Keppler BK. Searching for the magic bullet: anticancer platinum drugs which can be accumulated or activated in the tumor tissue. Anti-Cancer Agents Med. Chem 2007;7:55–73.

(13). Pasqualini R, Koivunen E, Ruoslahti E. A Peptide Isolated from Phage Display Libraries Is a Structural and Functional Mimic of an RGD-binding Site on Integrins. J. Cell Biol 1995;130:1189–1196. [PubMed: 7657703]

(14). Haubner R, Wester H-J, Burkhart F, Senekowitsch-Schmidtke R, Weber W, Goodman S, Kessler H, Schwaiger M. Glycosylated RGD-Containing Peptides: Tracer for Tumor Targeting and Angiogenesis Imaging with Improved Biokinetics. J. Nucl. Med 2001;42:326–336. [PubMed: 11216533]

(15). Bhagwat S, Lahdenranta J, Giordano R, Arap W, Pasqualini R, Shapiro L. CD13/APN is activated by angiogenic signals and is essential for capillary tube formation. Blood 2001;97:652–659. [PubMed: 11157481]

(16). Hansel W, Enright F, Leuschner C. Destruction of breast cancers and their metastases by lytic peptide conjugates in vitro and in vivo. Mol. Cell. Endocrinol 2007;260-262:183–189. [PubMed: 17101210]

(17). Leuschner C, Kumar CSSR, Hansel W, Hormes J. Targeting breast cancer cells and their metastases through luteinizing hormone releasing hormone (LHRH) receptors using magnetic nanoparticles. J. Biomed. Nanotechnol 2005;1:229–233.

(18). Nagy A, Schally AV. Cytotoxic analogs of luteinizing hormone-releasing hormone (LHRH): a new approach to targeted chemotherapy. Drugs Future 2002;27:359–370.

(19). Schally AV, Nagy A. Cancer chemotherapy based on targeting of cytotoxic peptide conjugates to their receptors on tumors. Eur. J. Endocrinol 1999;141:1–14. [PubMed: 10407215]

(20). Schally AV, Nagy A. New approaches to treatment of various cancers based on cytotoxic analogs of LHRH, somatostatin and bombesin. Life Sci 2003;72:2305–2320. [PubMed: 12639697]

(21). Pasqualini R, Koivunen E, Kain R, Lahdenranta J, Sakamoto M, Stryhn A, Ashmun R, Shapiro L, Arap W, Ruoslahti E. Aminopeptidase N Is a Receptor for Tumor-homing Peptides and a Target for Inhibiting Angiogenesis. Cancer Res 2000;60:722–727. [PubMed: 10676659]

(22). Arap W, Pasqualini R, Ruoslahti E. Cancer treatment by targeted drug delivery to tumor vasculature in a mouse. Science (Washington, D. C., 1883-) 1998;279:377–380.

(23). Anizon F, Boyle T, Fisher J, Kocienski P. Synthesis and characterisation of a Doxorubicin-CNGRC Peptide conjugate that target tumor Vasculature. Synthesis 2002;18:2733–2736.

(24). Zhang Z, Hatta H, Tanabe K, Nishimoto S.-i. A New Class of 5-Fluoro-2 -deoxyuridine Prodrugs Conjugated with aTumor-Homing Cyclic Peptide CNGRC by Ester Linkers: Synthesis,Reactivity, and Tumor-Cell–Selective Cytotoxicity. Pharm. Res 2005;22:381–389. [PubMed: 15835743]

(25). Hanahan D, Folkman J. Patterns and Emerging Mechanisms Review of the Angiogenic Switch during Tumorigenesis. Cell (Cambridge, Massachusetts) 1996;86:353–364.

(26). Bhagwat S, Petrovic N, Okamoto Y, Shapiro L. The angiogenic regulator CD13/APN is a transcriptional target of Ras signaling pathways in endothelial morphogenesis. Blood 2003;101:1818–1826. [PubMed: 12406907]

(27). Birkenkamp-Demtroder K, Christensen LL, Olesen SH, Frederiksen CM, Laiho P, Aaltonen LA, Laurberg S, Sorensen FB, Hagemann R, Orntoft TF. Gene expression in colorectal cancer. Cancer Res 2002;62:4352–4363. [PubMed: 12154040]

(28). Curnis F, Arrigoni G, Sacchi A, Fischetti L, Arap W, Pasqualini R, Corti A. Differential Binding of Drugs Containing the NGR Motif to CD13 Isoforms in Tumor Vessels, Epithelia, and Myeloid Cells. Cancer Res 2002;62:867–874. [PubMed: 11830545]

(29). Ikeda N, Nakajima Y, Tokuhara T, Hattori N, Sho M, Kanehiro H, Miyake M. Clinical Significance of Aminopeptidase N/CD13 Expression in Human Pancreatic Carcinoma. Cancer Res 2003;9:1503–1508.

(30). Shepherd F, Sridhar S. Angiogenesis inhibitors under study for the treatment of lung cancer. Lung Cancer 2003;41:63–72.

(31). Giguere C,M, Bauman N,M, Smith R,JH. New treatment options for lymphangioma in infants and children. Ann. Otol. Rhinol. laryngol 2002;111:1066–75. [PubMed: 12498366]

(32). Hashida H, Takabayashi A, Kanai M, Adachi M, Kondo K, Kohno N, Yamaoka Y, Miyake M. Aminopeptidase N is involved in cell motility and angiogenesis: its clinical significance in human colon cancer. Gastroenterology 2002;122:376–386. [PubMed: 11832452]

(33). Albericio F, Cases M, Alsina J, Triolo SA, Carpino LA, Kates SA. On the use of PyAOP, a phosphonium salt derived from HOAt, in solid-phase peptide synthesis. Tetrahedron Lett 1997;38:4853–4856.

(34). Aronov O, Horowitz A, Gabizon A, Gibson D. Folate-Targeted PEG as a Potential Carrier for Carboplatin Analogs. Synthesis and in Vitro Studies. Bioconjugate Chem 2003;14:563–574.

(35). Berners-Price SJ, Frenkiel TA, Frey U, Ranford JD, Sadler PJ. Hydrolysis products of cisplatin: pKa determinations via [1H, 15N] NMR spectroscopy. J. Chem. Soc., Chem. Commun 1992:789–91.

(36). Appleton TG, Hall JR, Ralph SF, Thompson CSM. NMR study of acid-base equilibria and other reactions of ammineplatinum complexes with aqua and hydroxo ligands. Inorg. Chem 1989;28:1989–93.

(37). Appleton TG, Berry RD, Davis CA, Hall JR, Kimlin HA. Reactions of platinum(II) aqua complexes. 1. Multinuclear (platinum-195, nitrogen-15, and phosphorus-31) NMR study of reactions between the cis-diammineaquaplatinum(II) cation and the oxygen-donor ligands hydroxide, perchlorate, nitrate, sulfate, phosphate, and acetate. Inorg. Chem 1984;23:3514–21.

(38). Palocsay FA, Rund JV. Reaction between 1,10-phenanthroline and platinum(II) compounds. I. Reaction in aqueous solution. Inorg. Chem 1969;8:524–8.

(39). Basolo F, Bailar JC Jr. Tarr BR. The stereochemistry of complex inorganic compounds. X. The stereoisomers of dichlorobis(ethylenediamine)platinum(IV) chloride. J. Am. Chem. Soc 1950;72:2433–8.

(40). Aggarwal S, Takada Y, Singh S, Myers JN, Aggarwal BB. Inhibition of growth and survival of human head and neck squamous cell carcinoma cells by curcumin via modulation of nuclear factor-kB signaling. Int. J. Cancer 2004;111:679–692. [PubMed: 15252836]

(41). Alnemri ES, Livingston DJ, Nicholson DW, Salvesen G, Thornberry NA, Wong WW, Yuan J. Human ICE/CED-3 protease nomenclature. Cell (Cambridge, Mass.) 1996;87:171.

(42). Dupere-Minier G, Hamelin C, Desharnais P, Bernier J. Apoptotic volume decrease, pH acidification and chloride channel activation during apoptosis requires CD45 expression in HPB-ALL T cells. Apoptosis 2004;9:543–51. [PubMed: 15314282]

(43). Roberts MJ, Bentley MD, Harris JM. Chemistry for peptide and protein PEGylation. Adv. Drug Delivery Rev 2002;54:459–476.

(44). Veronese FM, Pasut G. PEGylation, successful approach to drug delivery. Drug Discovery Today 2005;10:1451–1458. [PubMed: 16243265]

(45). Esposito P, Barbero L, Caccia P, Caliceti P, D'Antonio M, Piquet G, Veronese FM. PEGylation of growth hormone-releasing hormone (GRF) analogs. Adv. Drug Delivery Rev 2003;55:1279–1291.

(46). Milanesio M, Monti E, Gariboldi MB, Gabano E, Ravera M, Osella D. Trend in cytotoxic activity of a series of cis-[APtCl2] (A=ethylenediamine methylated at different positions) complexes. Inorg. Chim. Acta 2008;361:2803–2814.

(47). Gabano E, Colangelo D, Ghezzi AR, Osella D. The influence of temperature on antiproliferative effects, cellular uptake and DNA platination of the clinically employed Pt(II)-drugs. J. Inorg. Biochem 2008;102:629–635. [PubMed: 18037490]

(48). Bonetti A, Apostoli P, Zaninelli M, Pavanel F, Colombatti M, Cetto GL, Franceschi T, Sperotto L, Leone R. Inductively Coupled Plasma Mass Spectroscopy Quantitation of Platinum-DNA Adducts in Peripheral Blood Leukocytes of Patients Receiving Cisplatin- or Carboplatin-based Chemotherapy'. Clin. Cancer Res 1996;2:1829–1835. [PubMed: 9816137]

(49). Harris A, Yang X, Hegmans A, Povirk L, Ryan J, Kelland L, Farrell N. Synthesis, Characterization, and Cytotoxicity of a Novel Highly Charged Trinuclear Platinum Compound. Enhancement of Cellular Uptake with Charge. Inorg. Chem 2005;44:9598–9600. [PubMed: 16363817]

(50). Elferink F, van der Vijgh WJ, ten Bokkel Huinink WW, Vermorken JB, Klein I, Winograd B, Knobf MK, Simonetti G, Gall HE, McVie JG. Pharmacokinetics of ethylenediaminemalonatoplatinum(II) (JM-40) during phase I trial. Br. J. Cancer 1987;56:479–83. [PubMed: 3689665]

(51). Hydes PC, Russell MJH. Advances in platinum cancer chemotherapy. Advances in the design of cisplatin analogs. Cancer Metastasis Rev 1988;7:67–89. [PubMed: 3293834]

(52). Cullen KJ, Yang Z, Schumaker L, Guo Z. Mitochondria as a critical target of the chemotheraputic agent cisplatin in head and neck cancer. J. Bioenerg. Biomembr 2007;39:43–50. [PubMed: 17318397]

(53). Singh S, Chhipa RR, Vijayakumar MV, Bhat MK. DNA damaging drugs-induced down-regulation of Bcl-2 is essential for induction of apoptosis in high-risk HPV-positive HEp-2 and KB cells. Cancer Lett 2006;236:213–221. [PubMed: 15996812]

(54). Kumar, s.; Lavin, MF. The ICE family of cysteine proteases as effectors of cell death. Cell Death Differ 1996;3:255–267. [PubMed: 17180094]

(55). Chaoui D, Faussat A-M, Majdak P, Tang R, Perrot J-Y, Pasco S, Klein C, Marie J-P, Legrand O. JC-1, a sensitive probe for a simultaneous detection of P-glycoprotein activity and apoptosis in leukemic cells. Cytometry, B. Clin. Cytom 2006;70B:189–196. [PubMed: 16568474]

(56). Cepeda V, Fuertes MA, Castilla J, Alonso C, Quevedo C, Pérez JM. Biochemical Mechanisms of Cisplatin Cytotoxicity. Anti-Canc. Agents Med. Chem 2007;7:3–18.

(57). Fichtinger-Schepman AMJ, Van der Veer JL, Den Hartog JHJ, Lohman PHM, Reedijk J. Adducts of the antitumor drug cis-diamminedichloroplatinum(II) with DNA: formation, identification, and quantitation. Biochemistry 1985;24:707–13. [PubMed: 4039603]

(58). Eastman A. Reevaluation of interaction of cis-dichloro(ethylenediamine)platinum(II) with DNA. Biochemistry 1986;25:3912–15. [PubMed: 3741840]

(59). Johnson NP, Mazard AM, Escalier J, Macquet JP. Mechanism of the reaction between cis-$[PtCl_2(NH_3)_2]$ and DNA in vitro. J. Am. Chem. Soc 1985;107:6376–80.

(60). Erickson LC, Zwelling LA, Ducore JM, Sharkey NA, Kohn KW. Differential cytotoxicity and DNA crosslinking in normal and transformed human fibroblasts treated with cis-diamminedichloroplatinum(II). Cancer Res 1981;41:2791–4. [PubMed: 7195771]

(61). Strandberg MC, Bresnick E, Eastman A. The significance of DNA crosslinking to cis-diamminedichloroplatinum(II)-induced cytotoxicity in sensitive and resistant lines of murine leukemia L1210 cells. Chem.-Biol. Interact 1982;39:169–80. [PubMed: 7199396]

(62). Dijt FJ, Fichtinger-Schepman AMJ, Berends F, Reedijk J. Formation and repair of cisplatin-induced adducts to DNA in cultured normal and repair-deficient human fibroblasts. Cancer Res 1988;48:6058–62. [PubMed: 3167856]

(63). Kroemer G, Zamzami N, Susin SA. Mitochondrial control of apoptosis. Immunol. Today 1997;18:44–51. [PubMed: 9018974]

(64). Shimizu S, Eguchi Y, Kamiike W, Waguri S, Uchiyama Y, Matsuda H, Tsujimoto Y. Bcl-2 blocks loss of mitochondrial membrane potential while ICE inhibitors act at a different step during inhibition of death induced by respiratory chain inhibitors. Oncogene 1996;13:21–29. [PubMed: 8700549]

(65). Ly JD, Grubb DR, Lawen A. The mitochondrial membrane potential (Delta ym) in apoptosis; an update. Apoptosis 2003;8:115–128. [PubMed: 12766472]

(66). Pasini A, Zunino F. New cisplatin analogs: on the way to better carcinostatics. Angew. Chem 1987;99:632–41.

(67). Reedijk J, Fichtinger-Schepman AMJ, Van Oosterom AT, Van de Putte P. Platinum amine coordination compounds as anti-tumor drugs. Molecular aspects of the mechanism of action. Structure and Bonding (Berlin) 1987;67:53–89.

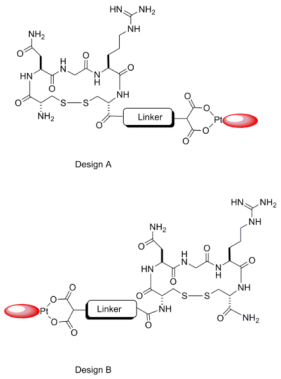

Figure 1.
CNGRC model conjugate with platinum pro-drug

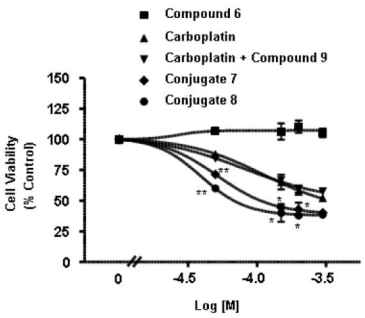

Figure 2. Cytotoxic effects of Pt complexes on PC-3 cells

Cyclic mPeg-CNGRC-mal (**6**), carboplatin, mixture of carboplatin and free peptide **9** (carboplatin + compound **9**), Pt-peptide conjugates; cyclic mPeg-CNGRC-Pt (**7**) and cyclic mPeg-CNGRC-Pten (**8**) on the proliferation of prostate cancer PC-3 (CD13 positive) cells. PC-3 cells were exposed to the compounds listed above and incubated for 48 h at different concentration. All points are a representative of mean +− SD of triplicate readings of the three independent experiment. *P = 0.0190 (carboplatin and conjugate **7**); P = 0.0126 (carboplatin and conjugate **8**); *P = 0.0407 (conjugate **7** and conjugate **8**). The difference is statistically significant as $P < 0.05$ at 150 μM concentrations. Statistical difference was determined by student's t test; one tailed by using Graph Pad Prism software version 5.0.

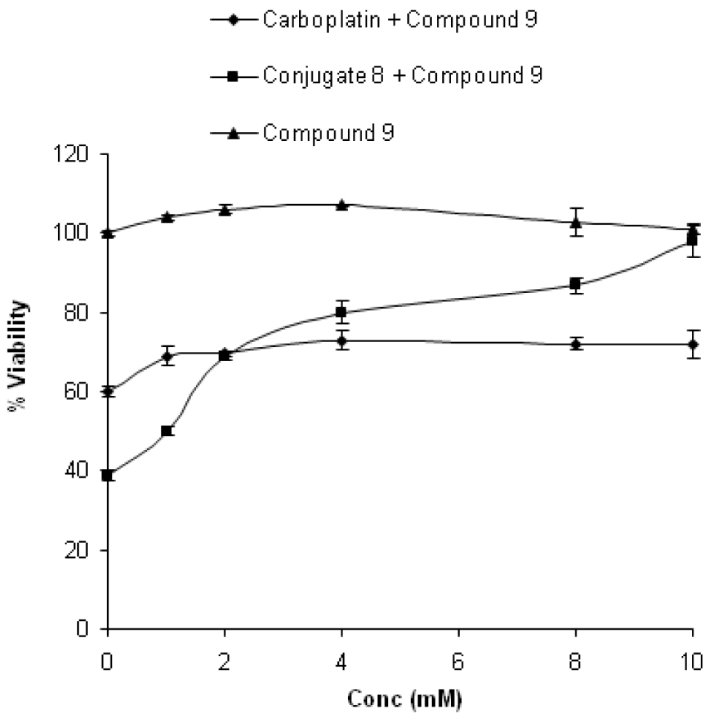

Figure 3. Role of the NRG peptide in cytoxicity

The effect of various concentrations of the free peptide **9** on 200 μM of carboplatin and conjugate **8**. Two thousand PC-3 cells were incubated with various concentrations of the free peptide mPeg-CNGRC (**9**) and 200 μM of carboplatin and conjugate **8** for 48 h. All points are a representative of mean +− SD of triplicate readings of the three independent experiment.

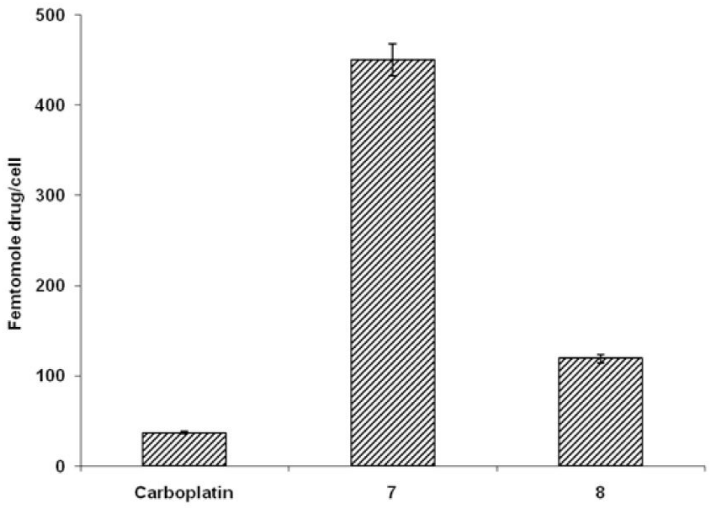

Figure 4. Platinum uptake of PC-3 (CD13 positive) cancer cells

One million cells were incubated with 200 μM carboplatin or Pt-peptide conjugate **7** or **8** for 24 h. Pt levels in the washed cells were measured by atomic absorption spectroscopy as described in the Experimental section. All points are a representative of mean +− SD of triplicate readings of the three independent experiment.

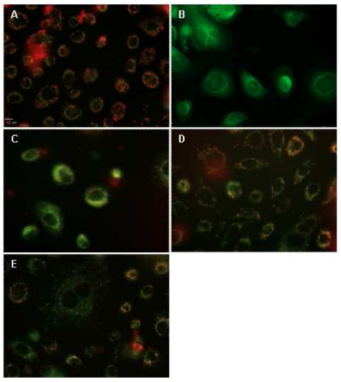

Figure 5. JC-1 Dye staining of cells treated with Pt-compounds

Fluorescence microscopy of cells that have been treated with various compounds, incubated for 48 h at 37 °C and then imaged by JC-1 staining after a further 30 min of incubation. Image **A** shows PC-3 cells, treated with RPMI media only. Image **B** shows PC-3 cells, treated with 50% DMSO. Image **C** shows PC-3 cells, treated with 200 μM of Pt-peptide conjugate **8** in RPMI media. Images **D** and **E** shows PC-3 cells incubated with a mixture of carboplatin/free peptide **9** (1:50) and carboplatin only (200 μM), respectively. Scale bar: 10 μm.

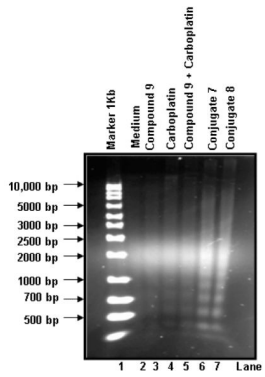

Figure 6. DNA fragmentation assay

PC-3 cells were treated with 5 μl of 1Kb DNA marker (lane 1), medium only (Lane 2), and 100 μM each of compound **9** alone (lane 3), carboplatin alone (lane 4), compound **9** + carboplatin (lane 5), conjugate **7** (lane 6) and conjugate **8** (lane 7) for 48 h. DNA was extracted and internucleosomal cleavage visualized on a 1.5% agarose gel. Image is representative of three independent experiment.

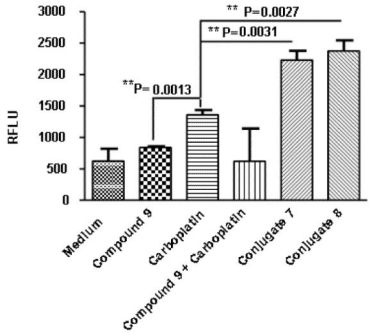

Figure 7. Caspase activation as a result of Pt-drug treatment

The apo-ONE homogenous caspase-3/7 assay where PC-3 cells (10,000 cells/well) in triplicate were treated with medium only and 100 μM concentration of the compound **9**, carboplatin alone, mixture of compound **9** and carboplatin, conjugate **7** and conjugate **8** for 24 h. After 24 h, the caspase activity was measured in the wells by adding 100 μl of the apo-ONE caspase-3/7 assay reagent. The cells were incubated for an additional hour at ambient temperature prior to recording fluorescence (485 Ex/527Em). The P values are statistically significant and calculated by student's t-test; one tailed.

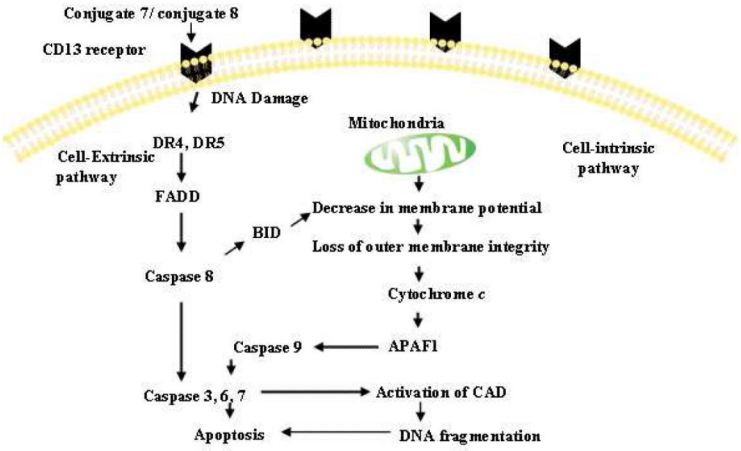

Figure 8.

Predicted pathways of apoptosis by conjugate 7 or 8. The cell-extrinsic apoptosis is engaged through death receptors (DR4 and DR5) and cell-intrinsic apoptosis is triggered through mitochondrial.

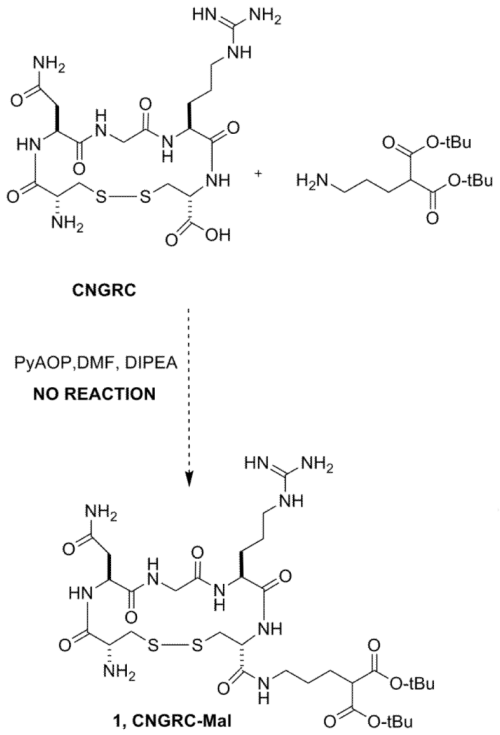

Scheme 1.
Coupling of CNGRC with di-tert-butyl 2-(3-aminopropyl)malonate.

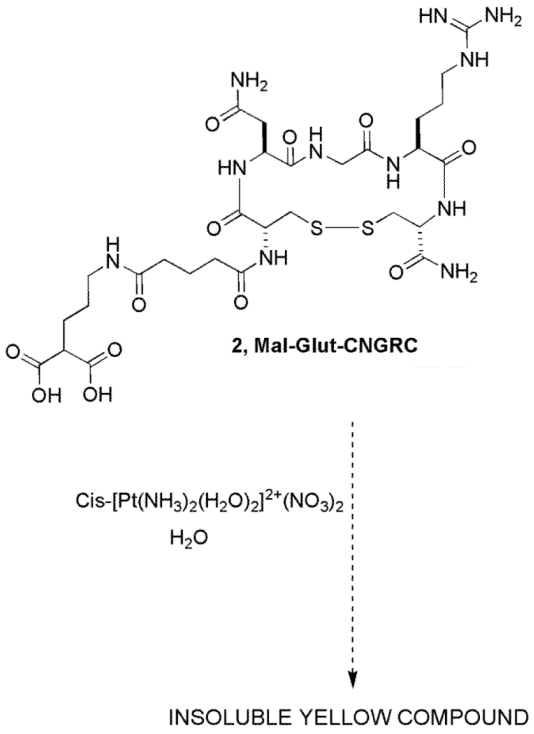

Scheme 2.
Platination reaction using Mal-Glut-CNGRC

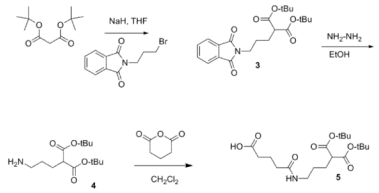

Scheme 3.
Synthesis of di-tert-butyl 2-(3-glutaricaminopropyl)malonate

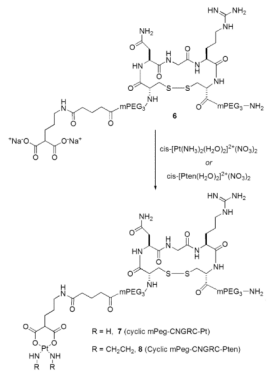

Scheme 4.
Formation of cyclic mPeg-CNGRC-Pt (**7**) and cyclic mPeg-CNGRC-Pten (**8**).